

Probing X-ray photoevaporative winds through their interaction with ionising radiation in cluster environments: the case for X-ray proplyds

C.J. Clarke^{1,3*} and J.E. Owen^{2,3}

¹*Institute of Astronomy, Madingley Rd, Cambridge, CB3 0HA, UK*

²*Canadian Institute for Theoretical Astrophysics, 60 St. George Street, Toronto, M5S 3H8, Canada.*

³*Nordita, Roslagstullsbacken 23, SE-10691, Stockholm, Sweden.*

21 August 2018

ABSTRACT

We show that if young low mass stars are subject to vigorous X-ray driven disc winds, then such winds may be rendered detectable in cluster environments through their interaction with ionising radiation from massive stars. In particular we argue that in the ONC (Orion Nebula Cluster) one expects to see of order tens of ‘X-ray proplyds’ (i.e. objects with offset ionisation fronts detectable through optical imaging) in the range 0.3–0.6pc from θ_1 C Ori (the dominant O star in the ONC). Objects at this distance lie outside the central ‘FUV zone’ in the ONC where proplyd structures are instead well explained by neutral winds driven by external Far Ultraviolet (FUV) emission from θ_1 C Ori. We show that the predicted numbers and sizes of X-ray proplyds in this region are compatible with the numbers of proplyds observed and that this may also provide an explanation for at least some of the far flung proplyds observed in the Carina nebula. We compare the sizes of observed proplyds outside the FUV region of the ONC with model predictions based on the current observed X-ray luminosities of these sources (bearing in mind that the current size is actually set by the X-ray luminosity a few hundred years previously, corresponding to the flow time to the ionisation front). We discuss whether variability on this timescale can plausibly explain the proplyd size data on a case by case basis. We also calculate the predicted radio free-free emission signature of X-ray proplyds and show that this is readily detectable. Monitoring is however required in order to distinguish such emission from non-thermal radio emission from active coronae. We also predict that it is only at distances more than a parsec from θ_1 C Ori that the free-free emission signature of such offset ionised structures would be clearly distinguishable from an externally driven ionised disc wind. We argue that the fortuitous proximity of massive stars in the ONC can be used as a beacon to light up internally driven X-ray winds and that this represents a promising avenue for observational tests of the X-ray photoevaporation scenario.

Key words: accretion, accretion discs - circumstellar matter - open clusters and associations: individual: Orion Nebula Cluster - planetary systems: protoplanetary discs - stars: pre-main sequence.

1 INTRODUCTION

The term ‘proplyd’ was originally coined by O’Dell et al (1993) as a contraction of ‘protoplanetary disc’ and has been applied to systems in star formation regions imaged either as bright rimmed cometary structures (in emission lines and continuum) or as dark ‘silhouette discs’. The vast majority of proplyds have been detected in the Orion Nebula Cluster, henceforth ONC (Lacques & Vidal 1979, Churchwell et al 1987, O’Dell et al 1993, Bally et al 2000) but there are also examples in other regions such as Carina (Smith

et al 2003), NGC 3603 (Brandner et al 2000) and Cyg OB2 (Wright et al 2012); see also Stecklum et al 1998, Yusef-Zadeh et al 2005, Balog et al 2006, Koenig et al 2008. The common feature of such regions is the presence of massive (OB) stars. This provides a bright background (in the case of silhouette discs) and is also consistent with the interpretation of bright cometary rims as stemming from the interaction between ionising radiation from these OB stars with the neutral material contained within the proplyd. The lack of a confining medium and the fact that the escape temperature at the ionisation front is much less than 10^4 K suggests that the gas is in a state of expansion at that point and this has been confirmed through emission line imaging (Henney & O’Dell 1999). The expansion

* E-mail: cclarke@ast.cam.ac.uk

timescale is so short however that this scenario requires that neutral gas is constantly re-supplied from some reservoir within the proplyds.

It is likely that observed proplyds are heterogeneous in nature. For example the ‘giant proplyds’ (i.e. those on a scale of $10^4 - 10^5$ AU) in NGC 3603 and Cyg OB2 are likely to be irradiated clumps of molecular gas (sometimes termed EGGs: embedded gaseous globules after Hester et al 1996). In other words, in these sources the reservoir of neutral material is distributed throughout the proplyd volume as would be expected if the object was pre-stellar or protostellar in nature. This interpretation is consistent with the lack of stars detected within some of these objects together with the rather high masses (of order a solar mass) detected via molecular line observations (Sahai et al 2012a,b). On the other hand, the bulk of proplyds in Orion (which are on a much smaller, ~ 100 AU scale) appear to be very different in nature since they typically contain stellar sources; discs, where detected in silhouette in these systems, are on a scale considerably less than the proplyd radius (Vicente & Alves 2005) and are moreover very low in mass (Mann & Williams 2010). In these objects it is necessary to posit a mechanism that lifts material from the relatively compact disc reservoir and brings it up to the ionisation front. Johnstone et al (1998) presented a simple and elegant framework for such objects in which material is lifted in a thermal wind driven by far-ultraviolet (FUV) radiation from the massive star that also provides the source of ionising photons. Such an interpretation is supported, for example, by the detection of molecular hydrogen $2.1\mu\text{m}$ emission (which is known to be pumped by FUV radiation) in a layer coincident with the disc surface (Chen et al 1998). Such models provide an excellent fit to spectroscopically determined mass loss rates in proplyds (Richling & Yorke 2000) and also broadly account for the observed proplyd size distribution. A critical aspect of such models is that FUV driven proplyds should only arise within a central zone of the cluster where the FUV radiation field is strong enough to drive a significant neutral wind. Outside this central ‘FUV zone’, molecular self-shielding limits the density of the neutral disc wind so that it can be readily penetrated by ionising photons. In this case, the ionisation front is expected to be virtually coincident with the disc surface rather than being spatially offset as in many observed proplyds. Störzer & Hollenbach (1999) estimated the radius of the FUV zone in Orion as being 0.3 pc and this is indeed consistent with the observed concentration of proplyds within this region (Bally et al 2000). However, there are at least ~ 10 proplyds in Orion that are well beyond the FUV zone of the most massive star ($\theta_1\text{C Ori}$) even in projection and which are likewise too far from other massive stars in the region to be good candidates for FUV driven winds (Vicente & Alves 2005). Smith et al (2003) similarly drew attention to a population of larger proplyds (size $\sim 900 - 2500$ A.U.) in Carina that are at surprisingly large distances (up to 40 pc) from the cluster core (note however that at least some of these may - unlike the Orion proplyds - fall into the EGG category described above: see Sahai et al 2012b for a demonstration of a high molecular gas mass in one such object).

Here we propose an alternative origin for some of the proplyds that are observed outside the central FUV zone of star-forming regions. We point out that if discs are subject to vigorous mass loss from winds driven by X-rays from their central stars (as proposed by Owen et al 2010, 2011, 2012) then the interaction between such winds and the ionising radiation from the dominant O star in the region should give rise to proplyd-like structures. We emphasise that the mass loss rates of X-ray driven winds are independent of the position in the cluster and depend only on the (time-averaged)

X-ray luminosity of each source. The role of the OB stars in the centre of the cluster is simply to ‘light up’ the surface of the wind at a distance that is - in the case of the more luminous X-ray sources - resolvable in HST images of Orion. In section 2 we discuss the X-ray properties of stars in the ONC and their variability and in Section 3 we assess the expected population of ‘X-ray proplyds’ and compare with observations. In Section 4 we consider the possible signatures of X-ray proplyds in the thermal radio continuum. Section 5 summarises our conclusions.

2 THE X-RAY PROPERTIES OF STARS IN THE ORION NEBULA CLUSTER

Before embarking on an analysis of how X-ray driven winds would affect the nature of objects imaged in the ONC we must consider the available data on the X-ray emission of young stars in the region. This has been well characterised by the Chandra Orion Ultradeep Project (COUP): Preibisch et al (2005) contains an analysis of the nearly 600 sources in Orion that are associated with stars that are well characterised in the optical and among which the X-ray detection rate is high ($> 97\%$). Kastner et al (2005) presented COUP data on the population of objects in Orion that are classified as proplyds (i.e. through association with cometary rims and/or silhouette structures). The detection rate in this sample (which overlaps the optical sample described above and which comprises ~ 140 objects) is considerably lower ($\sim 70\%$): the correlation between N_H and inclination in silhouette discs (noted by Kastner et al 2005) suggests that this is due to absorption rather than necessarily implying that proplyds are intrinsically weaker in the X-ray.

For clarity, we here stress that we do *not* define an X-ray proplyd as being a proplyd with a detected X-ray flux. Throughout this paper we use the term X-ray proplyd to denote *an object with an offset ionisation front that can be attributed to the interaction between ionising radiation from OB stars and a neutral wind driven off the disc by X-ray photoevaporation* (see Figure 1).

Before assessing whether there is any evidence for such a population in Orion we need to consider the amplitude of X-ray variability. When we come to calculate the expected radii of offset ionisation fronts as a function of X-ray luminosity (see equation (3), Section 3), the value of L_X that enters this calculation represents the X-ray luminosity (averaged over the thermal timescale at the flow base) that was emitted at a previous epoch separated in time by the timescale for the X-ray wind to propagate out to the ionisation front. This flow time is typically a few hundred years. We obviously have no information on the level of X-ray variability on these timescales. Although Favata et al (2004) found that some objects undergo variations of an order of magnitude or more on a timescale of years, Micela & Marino (2003) reported that the level of variability over periods from months to years is typically around 3–4 while Preibisch et al (2005) found a median change in X-ray luminosity of around a factor two between the COUP observations and those of Feigelson et al 2002 obtained 4 years earlier. The most recent variability study in Orion (Principe et al 2014) finds that variations by an order of magnitude or more are common over a four year period. Preibisch et al noted the large scatter in X-ray luminosities as a function of all variables (such as stellar mass, rotation period or Rossby number) and pointed out that this could in principle be due to large amplitude variability cycles. The magnitude of this scatter (i.e. more than two orders of magnitude in L_X at given stellar mass) however means that one would need to invoke large amplitude vari-

ability over a longer timescale than that covered by observational studies.

Given the lack of observational constraints on the level of X-ray variability over hundreds of years, we need to quantify the possible role of variability indirectly. In Section 3.1 we present a statistical approach (which assumes only that the X-ray luminosity function of the entire population is invariant over hundreds of years); in Section 3.2 we examine individual objects on a case by case basis, assessing the level of variability that is required in order for the observations and model predictions to agree.

3 THE SIZE OF X-RAY PROPLYDS AS A FUNCTION OF X-RAY LUMINOSITY AND DISTANCE TO THE IONISING STAR

We consider the situation where a star of X-ray luminosity L_X is located at a distance d from an ionising source with ionising photon output rate of $\Phi_{ion} \text{ s}^{-1}$. Following Owen et al (2012) we write

$$\dot{M}_w = 8 \times 10^{-9} L_{X30} M_{\odot} \text{ yr}^{-1} \quad (1)$$

(where L_{X30} is the X-ray luminosity in units of $10^{30} \text{ erg s}^{-1}$) noting that the mass loss rate is independent of the stellar mass and also of disc mass and radius, provided the latter is greater than 30 – 40 A.U. for a solar mass star (see Figure 4 of Owen et al 2010 for a cumulative mass loss profile from the disc, bearing in mind that the radial coordinate in this figure scales linearly with the stellar mass). The relevant X-ray luminosity is its value (averaged over a thermal timescale at the flow base: less than a decade, Owen et al 2010) at the time in the past (of order a few hundred years ago) when material currently on a ~ 100 A.U. scale was launched from the disc.

This X-ray driven wind is largely neutral but at some radius, R_{IF} , it becomes ionised by radiation from the dominant OB star in the cluster. Outward of R_{IF} the flow expands in a spherical transonic flow (i.e. with velocity of order the sound speed in the ionised medium). The ionisation front constitutes a contact discontinuity of the flow, requiring that the neutral flow entering the ionisation front is sub-sonic with respect to the neutral gas. In the absence of external ionisation, the X-ray driven wind becomes supersonic at radii less than 50 A.U. (i.e. on scales that are unresolvable even in the case of HST observations of the Orion Nebula Cluster). Observable proplyds must therefore correspond to the case where an already supersonic neutral flow has to undergo a shock in order to deliver neutral gas to the ionisation front with subsonic velocities. This is a qualitatively identical situation to that described by Johnstone et al (1998) in the case of ionising radiation interacting with FUV driven winds: clearly the details of the shock location will differ since the X-ray driven wind is considerably warmer (~ 4000 K) than that in the FUV driven flows (~ 1000 K). We show a schematic diagram of the flow in an X-ray proplyd in Figure 1.

What concerns us here is however the location of the ionisation front which is set by the requirement that the integrated recombination rate in the ionised flow matches the input of ionising photons (see Churchwell et al 1987 for a demonstration that the fraction of ionised photons that are additionally required to ionise the flux of neutral material into the ionisation front is a small fraction of the above). Since the density in the spherical transonic ionised wind falls with radius as r^{-2} , the integrated recombination rate per unit area scales as $n_i^2 R_{IF}$, where n_i is the density of ionised gas at R_{IF} (i.e. it is dominated by conditions close to the ionisation front). This condition fixes n_i as a function of R_{IF} and ionising flux. The

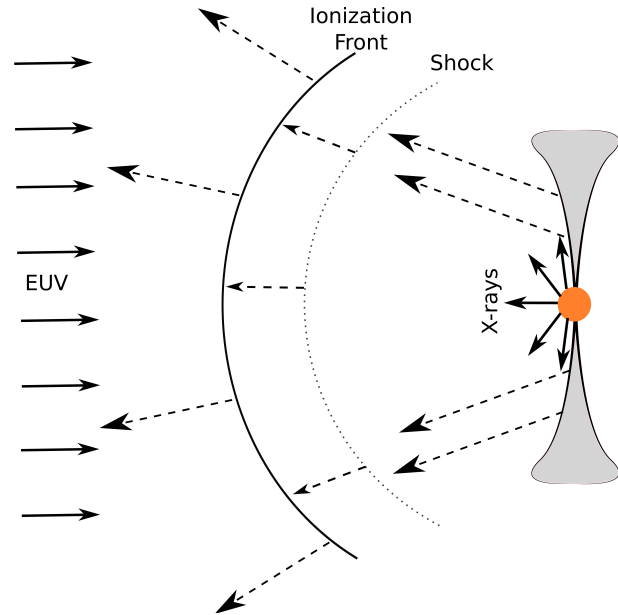


Figure 1. Schematic of flow in the case of an X-ray driven wind from a disc interacting with the ionising (EUV) radiation from a massive star.

mass loss rate from a spherical transonic ionised flow is however given by

$$\dot{M} = 4\pi R_{IF}^2 n_i \mu m_H c_s \quad (2)$$

where μ is the mean molecular weight, m_H is the mass of a proton and c_s is the sound speed in the ionised gas. Combined with the ionisation equilibrium requirement above, this fixes R_{IF} as a function of \dot{M} independent of the mechanism that delivers material to the ionisation front. We can thus readily adapt the formulation of Johnstone et al (1998) (where the FUV mass loss rate is determined by the requirement of a fixed neutral column) to the case of X-ray driven mass loss, which depends only on the X-ray luminosity of the source (see equation (1)). We thus have that the ‘chord diameter’ of the proplyd (which is equal to $2.6 \times R_{IF}$; Vicente & Alves 2005) is given by:

$$R_{cd} = 225 \text{ A.U.} \left(\frac{d_{pc}^2 L_{X30}^2}{\Phi_{ion49}} \right)^{1/3} \quad (3)$$

where d_{pc} is the distance from the ionising source in parsecs and Φ_{ion49} is the ionisation rate expressed in units of 10^{49} s^{-1} .

If we now apply this estimate to Orion (where Φ_{ion49} is about 1 in the case of the dominant OB star in the Trapezium cluster, θ_1 C Ori), we see that a proplyd with $L_{X30} \sim 1$ (which lies towards the upper end of the observed X-ray luminosity function for accreting stars in Orion; Preibisch et al 2005) would give rise to a proplyd of chord diameter ~ 100 A.U. if placed at the outer edge of the ‘FUV zone’ (i.e. at 0.3 pc from θ_1 C Ori). Since the cumulative X-ray luminosity function rises very steeply towards higher luminosities, it is unlikely that many of the observed proplyds in the FUV zone could instead be powered by internal X-ray driven winds (around 80% of stars observed by HST in this region are found to have proplyds that are considerably larger than this, i.e. with chord diameters of many hundreds of A.U.). On the other hand, models for proplyds in this region where disc winds are driven by FUV radiation from θ_1 C Ori can well account for the sizes of the observed proplyd distribution (Johnstone et al 1998). We thus concur with previous authors that the origin of the proplyd population within

0.3 pc of θ_1 C Ori is indeed likely to be a disc wind driven by external FUV radiation.

Although the majority of proplyds in the ONC are located in this central FUV zone, there are a number of proplyds at larger radius, even in projection. Around half of these may still be explainable by FUV heating by other OB stars in the region (i.e. θ_1 A Ori and θ_1 B Ori) although this has not been demonstrated. There are however at least 9 sources that are located in the range 0.3 – 0.6 pc in projection from θ_1 C Ori and which are likewise unlikely to receive significant FUV heating from the other OB stars. In Section 3.1 we assess whether the number and sizes of such objects are consistent with the expectations of X-ray driven proplyds, assuming that the X-ray luminosity function a few hundred years ago (when the current proplyd size was set) is identical to what it is now. This is a minimally constraining plausible assumption and so satisfying this test is a necessary condition for the viability of the model. In Section 3.2 we compare the observed X-ray fluxes of these 9 sources with the values that are required to explain their proplyd sizes and discuss whether any differences can be plausibly ascribed to variability.

3.1 Monte Carlo simulation of X-ray proplyds in the Orion Nebula Cluster

In what follows we adopt equation (3) in order to determine the expected chord diameter of a proplyd of given L_X and distance d from θ_1 C Ori. We populate stars in a spherically symmetric distribution centred on θ_1 C Ori which is consistent with the radial dependence of the observed surface density profile (Jones & Walker 1988, Hillenbrand 1997). We need to ensure that the density normalisation is consistent with the sample of objects contained in HST imaging campaigns of the ONC. Vicente & Alves record around 100 proplyds imaged in the central 0.3 pc of the cluster and comment that this is around 80% of the stars observed by HST in this region. Our piecewise power-law density distribution is thus normalised so that there are ~ 120 stars in this region:

$$\rho_* = 500 \text{pc}^{-3} \left(\frac{0.3 \text{pc}}{d} \right) \quad (4)$$

$$\rho_* = 500 \text{pc}^{-3} \left(\frac{0.3 \text{pc}}{d} \right)^2 \quad (5)$$

$$\rho_* = 45 \text{pc}^{-3} \left(\frac{\text{pc}}{d} \right)^5 \quad (6)$$

for the three regimes $d < 0.3 \text{pc}$, $0.3 < d < 1 \text{pc}$ and $d > 1 \text{pc}$ respectively; this roughly mimics the observed projected source distribution of Jones & Walker 1988 (see e.g. Figures 3 and 4 of Scally et al 2005). In our population synthesis modeling described below we also require that X-ray proplyds are only found in systems with discs and so multiply the above density profile by the observed disc fraction, f_d : we adopt $f_d = 0.8$ for $d < 0.3 \text{pc}$ and $f_d = 0.7$ for $d > 0.3 \text{pc}$ (Hillenbrand & Hartmann 1998).

For each star we select an X-ray luminosity from the COUP X-ray luminosity function for the ONC (Preibisch et al 2005); since X-ray proplyds can only be produced by stars with discs we adopt a parameterisation of the luminosity function for ‘accretors’ shown in Figure 17 of Preibisch et al 2005, limiting ourselves to stars with $L < 5L_\odot$, corresponding to stars less massive than $\sim 2M_\odot$. (Note that we do not use the XLF for proplyds partly because if the relative incompleteness of this sample in the X-rays - see discussion

in Section 2 - and also because we need for this exercise to use the XLF of the ‘parent’ disc bearing population rather than those that have been selected on account of resolvable structures). We parameterise the accretor XLF in three sections that are each individually flat in $\log(L_X)$, corresponding to the intervals 28 – 30, 30 – 30.3 and 30.3 – 31. The cumulative fractions of sources with $\log(L_X) < 30.$, < 30.3 and $< 31.$ are respectively 0.85, 0.96 and 1. Given that equation (3) implies that resolvable proplyds are associated with objects with $L_X > 10^{30}$, this analysis is evidently only sensitive to the parameterisation of the upper regions of the cumulative distribution function. For this exercise (in which we are estimating total numbers of predicted resolvable proplyds) we do not further sub-divide the Preibisch data by mass though we note that the upper envelope of the XLF declines rather steeply for spectral types of M4 and later. We will bring this consideration to bear when assessing the individual sources in Section 3.2 below.

We then evaluate the expected chord diameter based on equation (3). According to Vicente & Alves (2005), the proplyd census is complete only for structures larger than 150 A.U.. We thus record the projected position and chord diameters of all proplyds that are larger than this.

The result of this exercise is that we predict $\sim 20 - 30$ X-ray proplyds larger than 150 A.U. at projected distances of 0.3 – 0.6pc from θ_1 C Ori; within 0.3 pc we predict ~ 10 such proplyds. (As noted above, the latter is very small compared with the large number of proplyds (~ 100) observed in this central region and confirms the conventional interpretation of such objects as being driven by external FUV photoevaporation). The expected number of X-ray proplyds *outside* the central FUV zone is consistent with the numbers observed. The comparison with observations is complicated by the fact that it is unclear exactly how many of the proplyds observed outside the FUV zone of θ_1 C Ori can instead be attributed to FUV heating by other OB stars in the cluster. In Figure 2 we present the observed size distribution of proplyds that are possible candidate X-ray proplyds under two assumptions a) that all proplyds (~ 35) more than 0.3 pc from θ_1 C Ori are in this category and b) instead omitting from this sample those proplyds that are in the SW quadrant (i.e. in the vicinity of θ_1 A Ori and θ_1 B Ori). Under this conservative assumption ~ 9 proplyds are candidate X-ray proplyds (see Table 1) and these are described by the bold histogram in Figure 2. We see that the predicted numbers and size distributions of X-ray proplyds are well bracketed by the observations.

The Monte Carlo analysis has therefore demonstrated that the numbers and sizes of proplyds observed in this region are broadly consistent with those predicted by the X-ray proplyd model.

3.2 Assessing individual candidate X-ray proplyds.

Given this success in terms of predicting over-all numbers of proplyds with projected separations in the range 0.3 – 0.6 pc we now proceed to examining individual sources. We will investigate whether the sizes of observed proplyds in this region are consistent with those predicted from their current X-ray luminosities and, if not, what level of variability would need to be invoked in order to bring the figures into agreement.

As explained in Section 2, we first assume that the chord diameter of offset ionisation fronts can be calculated from equation (3), with L_X given by the *observed* X-ray luminosity of each source. In Table 1 we detail 9 proplyds that lie outside the central FUV zone of θ_1 C Ori (i.e. outside a projected radius of 0.3 pc and which are not in the SW quadrant where they may be ionised instead by θ_1 A Ori and θ_1 B Ori). In 8/9 of the sources there is an optical counterpart

and we list, where available, the spectral type as given by Getman et al (2005). Observed chord diameters are obtained from Vicente & Alves (2005). 7/9 of the sources are detected in X-rays and for these sources we list L_X from Kastner et al (2005) and the minimum predicted chord diameter (R_{pm}) for the X-ray proplyd model, calculated using equation (3). The value of R_{pm} is somewhat underestimated since we set the distance from θ_1 C Ori equal to the projected distance: on average this will cause the predicted sizes to be under-estimated by a factor of order unity given the $d^{2/3}$ scaling of equation (3). Note that, in contrast, the Monte Carlo analysis of Section 3.1 explicitly models how projection effects influence the expected sizes distribution but that this approach is not applicable on an object by object basis.

We also list for each source the value of $\log L_{X,m}$ which is the value of X-ray luminosity required to bring the predicted and observed proplyd sizes into agreement in the case that the 3D distance of the source from θ_1 C Ori is equal to its projected distance. The final column lists the ratio of $L_{X,m}$ to the bolometric luminosity of the source which is derived, where available, from Getman et al 2005. The actual value of the luminosity required is actually $L_{X,m}/\tilde{r}$ where \tilde{r} is the unknown ratio of the 3D distance to θ_1 C Ori and its projected value. For the assumed cluster density profile, the expectation value of \tilde{r} is about 1.4 and its maximum value is ~ 3 .

There is one source (172-135) where the non-detection in X-rays can be explained by it being a silhouette disc viewed close to edge on: the poor constraint on the intrinsic X-ray luminosity makes it unsuitable for our analysis. Among the remaining 8 sources, there are two where the observed X-ray luminosity is consistent with that required to explain the proplyd size (invoking at most modest projection corrections): these two sources are 073-227 and 140-1952. There are three sources (005-514, 102-021 and 152-738) where the combination of projection effects and less than order of magnitude variations can reconcile the model predictions with observations. The final three objects (066-652, 131-046 and 097-125) all require more than order of magnitude enhancement of the X-ray flux a few hundred years ago compared to its current value. Note that the fact that we would require all the sources to have been as bright or brighter in the X-ray than they are now is not *per se* an argument against the model: we would expect resolvable proplyds to be objects that selectively populate the upper end of the XLF at the relevant epoch and thus, on average, that they should be fainter now than previously. On the other hand, we can ask whether the X-ray luminosity that we need to invoke in the past is a reasonable value given typical values of L_X/L_{bol} in young stars as a function of spectral type. The final column shows that the values required are of order 10^{-3} ; such values are found in around 10% of young stars in the ‘accretor’ category, regardless of spectral type (Preibisch et al 2005).

We therefore conclude that at least some of the sample are compatible with being X-ray proplyds: the number that fall into this category depends on the amplitude of X-ray variability that one is prepared to invoke on timescales of hundreds of years. It has to remain a matter of speculation whether individual sources may (as in the most extreme case, 066-652) be as much as a factor hundred fainter currently than they were in the past; we however note that even here the implied L_X/L_{bol} value at a previous epoch was not extreme. When considering the likelihood that these objects are indeed X-ray proplyds it needs to be borne in mind that no other models have been proposed to explain offset ionisation fronts at such large distances from θ_1 C Ori.

Since we have shown in Section 3.1 that the model predicts a roughly correct number of resolvable X-ray proplyds over-all

Table 1. Predicted and observed properties of candidate X-ray proplyds. ST is the spectral type, R_{cd} is the chord diameter in A.U. and R_{pm} is a lower limit to the predicted chord diameter from the model (equation (3)) under the assumption that the 3D distance to θ_1 C Ori is the projected distance and the relevant X-ray luminosity is the observed value (listed in the successive column). $L_{X,m}$ (next column) is the X-ray luminosity that is required in order for the model to match the data in the case that the 3D distance to θ_1 C Ori is the projected value; the actual predicted X-ray luminosity required is typically a few tenths of a dex smaller than this on account of projection effects (see text). The final column (\tilde{L}) lists the logarithmic ratio of $L_{X,m}$ to the bolometric luminosity of the source. ^a The non-detection of this source in the X-ray is explicable in terms of it being a nearly edge-on silhouette disc.

Name	ST	R_{cd}	R_{pm}	$\log(L_X)$	$\log(L_{X,m})$	$\log(\tilde{L})$
005 – 514	K6	414	137	29.9	30.6	–2.5
066 – 652	M4.5	612	34	29.0	30.9	–2.3
072 – 135 ^a	–	472	–	–	30.8	–
073 – 227	M2 – M4	207	142	30.1	30.3	–2.7
097 – 125	M3.5	207	32	29.1	30.3	–3.0
102 – 021	M3.5	155	39	29.2	30.1	–2.7
131 – 046	–	270	–	–	30.5	–
140 – 1952	lateG	228	219	30.3	30.3	–3.0
152 – 738	–	243	73	29.5	30.3	–

(while Table 1 implies that most of the observed proplyds need to have been more X-ray luminous in the past than they are now) it is a necessary corollary that there should be objects that are currently X-ray bright but which do not show resolvable proplyd structure. Examples of such objects are found among pure silhouette discs (i.e. those that do *not* show a resolvable offset ionisation front) since in some of these the current X-ray luminosities are sufficient to produce a detectable offset ionisation front (e.g. 183 – 405)¹ Although we need to argue that X-ray variability disrupts any strong correlation between X-ray luminosity and resolvable proplyd structure, there is some weak evidence for a residual association: among our candidate X-ray proplyds (i.e. the objects listed in Table 1), 7/9 are detected in X-rays whereas among the pure silhouette discs this figure is only 8/16 (Kastner et al 2005).

4 THE RADIO EMISSION SIGNATURE OF X-RAY PROPLYDS

We now consider the free-free emission signature that we expect to be associated with the externally ionised X-ray proplyd population (see Pascucci et al 2012, 2014, Owen et al 2013 for a discussion of the free-free emission signatures expected from photoevaporative flows in the absence of external ionisation). For now we only consider the emission from ionised material in the wind external to R_{IF} . For reference we note that X-ray driven photoevaporative flows also generate an intrinsic free-free flux within an A.U. associated with ionisation by EUV photons from the star; scaling the

¹ There may however be a detectability issue in edge-on silhouettes which does not affect conventional (FUV driven) proplyds. While in the FUV case the wind is launched from regions extending to the disc’s outer edge and the ionisation front is always somewhat larger than the disc, optical depth effects in the X-ray driven case restrict the wind launching region to < 50 A.U. *regardless of the disc size*. Due to disc flaring, it may be difficult to detect compact (~ 100 A.U.) scale ionisation fronts in the case of large, edge-on silhouettes (as in 114 – 426 and 053 – 717).

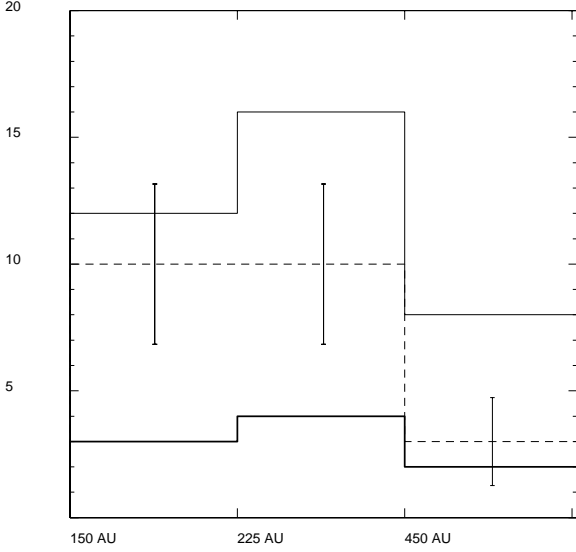


Figure 2. The numbers of proplyds as a function of size in the ONC. The upper histogram refers to the 35 proplyds in the ONC that are in the range 0.3 to 0.6 pc from θ_1 C Ori. The lowest (bold) histogram considers the same sample but omitting the 24 objects in this category that may arguably be in the FUV zone of θ_1 A Ori or θ_1 B Ori. The dashed histogram is the result of the population synthesis exercise for the predicted numbers of X-ray proplyds in the radial range 0.3 to 0.6 pc in projection. The three size bins refer to chord diameters in the range 150 – 225 A.U., 225 – 450 A.U. and > 450 A.U.. Observational data from the compilation of Vicente & Alves (2005).

results of Owen et al (2013) to the distance of Orion and assuming a ratio of ionising photon output to X-ray luminosity of 10^{11} erg^{-1} , we expect the *intrinsic* flux density at 2 cm to be:

$$L_{ff,int} = 0.005 L_{X30} \text{ mJy} \quad (7)$$

This value is comfortably less than the levels arising from external ionisation (equations (10) and (11) below) and so we do not consider free-free emission from internal ionisation further. In order to calculate the expected free-free flux from *external* ionisation of X-ray driven winds, we employ equation (2) of Garay et al (1987) for optically thin thermal emission ²:

$$\left[\frac{S_\nu}{\text{mJy}} \right] = 3.4 \left[\frac{\nu}{\text{GHz}} \right]^{-0.1} \left[\frac{T_e}{10^4 \text{ K}} \right]^{-0.35} \left[\frac{\text{VEM}}{10^{57} \text{ cm}^{-3}} \right] \left[\frac{D}{\text{kpc}} \right]^{-2} \quad (8)$$

where D is the distance to the ONC and the volume emission measure for a spherical constant velocity wind is given by:

$$\text{VEM} = 4\pi n_i^2 R_{IF}^3 \quad (9)$$

Combining this also with equations (2) and (3) (recalling that $R_{cd} = 2.6R_{IF}$ and assuming $T_e = 10^4 \text{ K}$ and $D = 450 \text{ pc}$) we then obtain that the flux density at 15 GHz (2 cm) is:

$$\left[\frac{S_{15\text{GHz}}}{\text{mJy}} \right] = 0.06 L_{X30}^{4/3} d_{pc}^{-2/3} \quad (10)$$

² Note that the optical depth is proportional to the integral of n^2 along the line of sight which, in ionisation equilibrium, depends only on the ionising flux, independent of n ; we thus find that the predicted emission is *optically thin* for wavelengths $< 15 \text{ cm} \Phi_{49}^{-1/2.1} d_{pc}^{2/2.1}$, independent of X-ray luminosity.

In Figure 3 we convert this expression into the equivalent radio luminosity (L_{ff} in $\text{erg s}^{-1} \text{ Hz}^{-1}$) and plot the predicted relationship between L_{ff} and L_X for a range of values of d (neglecting X-ray variability: see Section 3.2). We however need to take account of the fact that - even in the absence of any significant neutral (X-ray driven) wind - objects outside the central FUV zone are expected to sustain ionised winds associated with direct evaporation by EUV (ionising) photons from θ_1 C Ori: naturally such winds do not produce a proplyd signature (because the ionisation front is coincident with the disc surface) but there is an associated free-free emission signature. Adopting the mass loss rates for such winds as predicted by Johnstone et al (1998) we find:

$$\left[\frac{S_{15\text{GHz}}}{\text{mJy}} \right]_{EUV} = 0.06 R_{d100}^2 d_{pc}^{-2} \quad (11)$$

where R_{d100} is the disc radius normalised to 100 A.U. (note that in this case the wind is driven over the entire extent of the disc and hence the VEM depends on the disc radius, in contrast to the case of X-ray driven winds: see footnote 1) The free-free emission levels predicted by equation (10) thus only apply where these exceed the ‘floor’ EUV level predicted by equation (11). In Figure 3 we mark on each track the floor levels of radio emission corresponding to disc radii of 50 and 100 A.U. by open and filled triangles respectively.

We also plot (open circles) the Güdel & Benz (1993) relationship between X-ray and radio luminosity based on observations of weak line T Tauri stars and other disc-less but active objects. This characteristic locus is generally interpreted in terms of the generation of both X-ray and (non-thermal) radio emission in the stellar corona. The solid dots and open squares are derived from the VLA survey of the innermost region of the ONC by Zapata et al (2004), with the latter symbols corresponding to optical proplyds where the X-ray luminosities are taken from Kastner et al (2005). We emphasise that this data cannot be contrasted with our model predictions because all the sources in the VLA survey have projected distances that place them within the central FUV zone. The data however demonstrates that the bulk of non-proplyd sources lie along the Güdel-Benz relation (as expected in the case of disc-less stars) whereas most optical proplyds are indeed well offset to the right of this relation (see Forbrich & Wolk 2013), consistent with there being an additional thermal component as argued by Churchwell et al 1987, Garay et al 1988. The free-free flux density of the brightest proplyds in the central FUV zone of the ONC is several 10s of mJy and thus much greater than what we are predicting in the case of X-ray proplyds. (In the case of a transonic spherical ionised wind, the radio luminosity scales with the square of the mass loss rate and inversely with the radius of the ionisation front: the proplyds in the ‘FUV zone’ have high mass loss rates and are relatively compact and are thus considerably brighter in the radio than we predict for the putative population of X-ray proplyds at larger radius in the cluster).

The predicted level of thermal radio emission from X-ray proplyds is in the range 0.1 – 1 mJy and would be readily detectable in the ONC. There are however two factors (confusion with non-thermal emission in X-ray luminous stars and also confusion with emission from ionised winds driven by θ_1 C Ori) that complicate the interpretation of sources detected along the predicted loci. Since our predicted thermal emission signature (equation (10)) scales as $L_X^{4/3}$ (at fixed distance from θ_1 C Ori), it defines a relation that is roughly parallel to the Güdel & Benz relation. At distances $> 0.3 \text{ pc}$ from θ_1 C Ori (which is the region in which we expect X-ray proplyds to take over from FUV driven proplyds) the expected relation

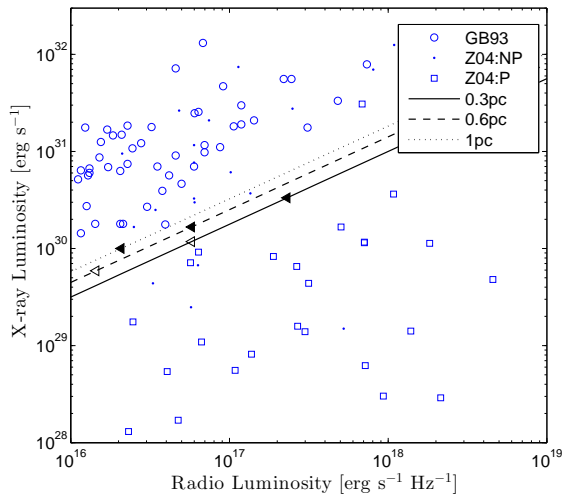


Figure 3. The predicted relationship between 3.6 cm radio luminosity (in $\text{erg s}^{-1} \text{Hz}^{-1}$) and X-ray luminosity (in erg s^{-1}) for a range of distances from θ_1 C Ori. The open and filled triangles on each track correspond to the ‘floor’ values of radio emission (for disc radii of 50 and 100 A.U. respectively) that are expected from ionised winds driven by θ_1 C Ori in the absence of internal X-ray driven winds. The open circles are the data of Güdel & Benz (1993), while the remaining points are from the survey of Zapata et al (2004) for the inner regions (‘FUV zone’) of the ONC, with squares and solid dots denoting sources that are (Z04:P) or are not (Z04:NP) identified with imaged proplyd systems. X-ray luminosities for the proplyd systems derive from Kastner et al (2005)

is close to the bottom of the Güdel & Benz relation. We thus conclude that the thermal emission from such objects would be hard to distinguish from non-thermal (coronal) emission based on radio luminosities alone. Unfortunately, multi-wavelength data cannot on its own discriminate between these possibilities since the spectral index for non-thermal gyrosynchrotron emission can vary over a wide range depending on the energy spectrum of the electrons involved (Güdel 2002). Instead the best prospect for disentangling the relative contributions from thermal and non-thermal free-free emission is via monitoring, since non-thermal emission is notably variable on timescales of months to years (Zapata et al 2004).

The other factor which complicates the interpretation of radio emission in terms of an X-ray driven wind is the expected ‘floor’ value (equation 11) produced by winds driven by EUV emission from θ_1 C Ori. Comparison of equations (10) and (11) show that the floor value drops more steeply with distance from θ_1 C Ori than does the X-ray wind radio signature at fixed X-ray luminosity. Thus the unambiguous detection of X-ray driven winds is most readily achieved at relatively large distances (a parsec or more) from θ_1 C Ori.

The detection of thermal emission of the expected magnitude in sources more than a parsec from θ_1 C Ori would be strong evidence in favour of X-ray driven winds interacting with the external ionising flux from θ_1 C Ori³.

³ From equations (7) and (10) the thermal emission from this interaction exceeds that arising from the inner regions of the X-ray driven wind itself provided that $L_{X30} > 10^{-3} d_{pc}^2$

5 CONCLUSIONS

We have shown that the interaction between ionising radiation from massive stars and (internally driven) X-ray heated disc winds should give rise to extended structures that we term ‘X-ray proplyds’. Even in the closest suitable environment (the ONC), resolvable X-ray proplyds would correspond only to objects at the upper end of the X-ray luminosity function (note that the relevant X-ray luminosity is its value at a time in the past corresponding to typical flow times from the disc to the ionisation front (hundreds of years); this does not necessarily correspond to current X-ray luminosity: see Section 3.2). Even in luminous X-ray sources, however, the predicted mass loss rates are less than the rates of mass loss driven by external FUV heating in the close vicinity of massive stars. In the case of the ONC, this means that the majority of proplyds (which reside within 0.3 pc of the central OB star θ_1 C Ori) are indeed FUV driven as argued by previous authors; however FUV heating is ineffective at larger distances from θ_1 C Ori and it is here that we expect to see a population of X-ray proplyds.

We have demonstrated that the numbers and sizes of proplyds observed in the ONC outside the central FUV zone is compatible with the expectations of the X-ray proplyd model provided that we make the reasonable assumption that the X-ray luminosity function was the same a few hundred years ago (when the present day mass loss at the ionisation front was set) as it is now. Turning to predictions for individual objects with measured current X-ray fluxes we find a mixed picture - in some cases (2/8) the proplyd size is a good match to that predicted whereas in others the required X-ray flux is significantly higher than it is now. We require greater (less) than order of magnitude variations in 3/8 (3/8) objects: note that order of magnitude variations in X-ray flux are commonly observed in disc bearing pre-main sequence stars on timescales of years (Principe et al 2014). We also note that at least some of the large proplyds in Carina (with scales of 10^3 A.U.; Smith et al 2003) observed up to 40 pc from the main ionising source in this region (η Carina) are also compatible with being X-ray proplyds. Future radiation-hydrodynamical modeling will indicate further avenues for observational characterisation of X-ray proplyds through generation of predicted line emission profiles and synthetic images.

We also show that X-ray proplyds are predicted to produce thermal radio emission at levels that are readily detectable in the ONC. However, the predicted scaling between free-free radio luminosity and X-ray luminosity ($L_{ff} \propto L_X^{4/3}$ at fixed distance from the ionising source) is similar to the trend observed in disc-less active stars (Güdel & Benz 1993) and is indeed only modestly offset towards higher radio luminosities. Monitoring of the emission levels on timescales of months to years is therefore required in order to disentangle thermal and non-thermal contributions. We also show that in order to distinguish the signature of X-ray proplyds from that of a wind driven purely by the ionising radiation from θ_1 C Ori, it is necessary to examine sources at > 1 pc from θ_1 C Ori.

Clearly we obtain the greatest model discrimination in the case that we can detect thermal radio emission *and* measure the spatial offset of the ionisation front since in that case it is possible to evaluate the mass loss rate in the wind (assuming a typical transonic flow velocity) independent of any assumptions about the ionising flux at the ionisation front. As already noted, the population of objects outside the central FUV zone with optically detected offset ionisation fronts is small (10s of objects) and corresponds (in our model) to objects with the largest X-ray luminosities a few hundred years ago. JWST offers the prospect of being able to image

the large population of objects with more compact structures that we predict.

6 ACKNOWLEDGMENTS

We would like to acknowledge the Nordita program on Photo-Evaporation in Astrophysical Systems (June 2013) where this work was initiated and are grateful to Will Henney for a question that sparked this investigation. We gratefully acknowledge the referee, Joel Kastner, for comments that have improved the analysis presented here and also thank Fred Adams, Richard Alexander and Ilaria Pascucci for useful discussions. JEO acknowledges support through the IOA's STFC funded Visitor Programme. This work has been supported by the DISCSIM project, grant agreement 341137 funded by the European Research Council under ERC-2013-ADG.

REFERENCES

- Alexander R. D., Clarke C. J., Pringle J. E., 2005, *MNRAS*, 358, 283
- Bally J., O'Dell C. R., McCaughrean M. J., 2000, *AJ*, 119, 2919
- Balog Z., Rieke G. H., Su K. Y. L., Muzerolle J., Young E. T., 2006, *ApJ*, 650, L83
- Brandner W., et al., 2000, *AJ*, 119, 292
- Chen H., Bally J., O'Dell C. R., McCaughrean M. J., Thompson R. L., Rieke M., Schneider G., Young E. T., 1998, *ApJ*, 492, L173
- Churchwell E., Felli M., Wood D. O. S., Massi M., 1987, *ApJ*, 321, 516
- Favata F., Micela G., Baliunas S. L., Schmitt J. H. M. M., Güdel M., Harnden F. R., Jr., Sciortino S., Stern R. A., 2004, *A&A*, 418, L13
- Forbrich J., Wolk S. J., 2013, *A&A*, 551, AA56
- Getman K. V., et al., 2005, *ApJS*, 160, 319
- Garay G., Moran J. M., Reid M. J., 1987, *ApJ*, 314, 535
- Güdel M., 2002, *ARA&A*, 40, 217
- Guedel M., Benz A. O., 1993, *ApJ*, 405, L63
- Henney W. J., O'Dell C. R., 1999, *AJ*, 118, 2350
- Hester J. J., et al., 1996, *AJ*, 111, 2349
- Hillenbrand L. A., 1997, *AJ*, 113, 1733
- Hillenbrand L. A., Hartmann L. W., 1998, *ApJ*, 492, 540
- Johnstone D., Hollenbach D., Bally J., 1998, *ApJ*, 499, 758
- Jones B. F., Walker M. F., 1988, *AJ*, 95, 1755
- Kastner J. H., Franz G., Grosso N., Bally J., McCaughrean M. J., Getman K., Feigelson E. D., Schulz N. S., 2005, *ApJS*, 160, 511
- Koenig X. P., Allen L. E., Kenyon S. J., Su K. Y. L., Balog Z., 2008, *ApJ*, 687, L37
- Laques P., Vidal J. L., 1979, *A&A*, 73, 97
- Mann R. K., Williams J. P., 2010, *ApJ*, 725, 430
- Micela G., Marino A., 2003, *A&A*, 404, 637
- O'dell C. R., Wen Z., Hu X., 1993, *ApJ*, 410, 696
- Owen J. E., Ercolano B., Clarke C. J., Alexander R. D., 2010, *MNRAS*, 401, 1415
- Owen J. E., Ercolano B., Clarke C. J., 2011, *MNRAS*, 412, 13
- Owen J. E., Clarke C. J., Ercolano B., 2012, *MNRAS*, 422, 1880
- Owen J. E., Scaife A. M. M., Ercolano B., 2013, *MNRAS*, 434, 3378
- Pascucci I., Gorti U., Hollenbach D., 2012, *ApJ*, 751, LL42
- Pascucci I., Ricci L., Gorti U., Hollenbach D., Hendlner N. P., Brooks K. J., Contreras Y., 2014, *ApJ*, 795, 1
- Preibisch T., et al., 2005, *ApJS*, 160, 401
- Principe D. A., Kastner J. H., Grosso N., Hamaguchi K., Richmond M., Teets W. K., Weintraub D. A., 2014, *ApJS*, 213, 4
- Richling S., Yorke H. W., 2000, *ApJ*, 539, 258
- Sahai R., Morris M. R., Claussen M. J., 2012, *ApJ*, 751, 69
- Sahai R., Güsten R., Morris M. R., 2012, *ApJ*, 761, LL21
- Scally A., Clarke C., McCaughrean M. J., 2005, *MNRAS*, 358, 742
- Smith N., Bally J., Morse J. A., 2003, *ApJ*, 587, L105
- Stecklum B., Henning T., Feldt M., Hayward T. L., Hoare M. G., Hofner P., Richter S., 1998, *AJ*, 115, 767
- Störzer H., Hollenbach D., 1999, *ApJ*, 515, 669
- Vicente S. M., Alves J., 2005, *A&A*, 441, 195
- Wright N. J., Drake J. J., Drew J. E., Guarcello M. G., Gutermuth R. A., Hora J. L., Kraemer K. E., 2012, *ApJ*, 746, LL21
- Yusef-Zadeh F., Biretta J., Geballe T. R., 2005, *AJ*, 130, 1171
- Zapata L. A., Rodríguez L. F., Kurtz S. E., O'Dell C. R., 2004, *AJ*, 127, 2252